

## Upconversion

# Single-Band Upconversion Emission in Lanthanide-Doped KMnF<sub>3</sub> Nanocrystals\*\*

Juan Wang, Feng Wang, Chao Wang, Zhuang Liu, and Xiaogang Liu\*

The preparation of upconversion (UC) nanocrystals that exhibit anti-Stokes emission is important for applications in fields as diverse as photonics, photovoltaics, biological imaging, and therapeutics.<sup>[1–4]</sup> In particular, there has been an increasing focus on the synthesis of nanocrystals with tunable UC emission from ultraviolet to near-infrared through doping with lanthanide ions.<sup>[5]</sup> However, the synthesis of nanocrystals featuring single-band UC with high chromatic purity remains a formidable challenge, as lanthanide ions generally have more than one metastable excited state.<sup>[6]</sup> In principle, these lanthanide-doped nanocrystals display multipeak emission profiles.

Recently, several attempts have been made to obtain high purity of single-band UC red emission attractive for anti-counterfeiting and color display applications.<sup>[7]</sup> For example, high red-to-green (R/G) emission ratio can be achieved by increasing the concentration of Yb<sup>3+</sup> in Yb/Er co-doped NaYF<sub>4</sub> nanoparticles.<sup>[8]</sup> In addition, Yb/Er co-doped MnF<sub>2</sub> and KMnF<sub>3</sub> nanoparticles have shown substantially enhanced R/G emission ratios because of the energy transfer between the Er<sup>3+</sup> and Mn<sup>2+</sup>.<sup>[9]</sup> However, a general method for providing single-band red emission has not been conclusively established. Herein, we report a novel oil-based procedure for the synthesis of lanthanide-doped KMnF<sub>3</sub> nanocrystals with only single-band UC emissions from Er<sup>3+</sup>, Ho<sup>3+</sup>, and Tm<sup>3+</sup> dopants, respectively. Importantly, we observe that the single-band feature is independent of dopant concentration, pump power, and temperature. We also show that these nanocrystals can serve as ideal optical biolabels for deep-tissue imaging without the constraints associated with conventional multi-peak UC nanocrystals.

The lanthanide-doped KMnF<sub>3</sub> nanocrystals for the present study were prepared in three steps according to a

modified literature procedure.<sup>[10]</sup> In the first step, lanthanide and manganese precursors were first dissolved in oleic acid at 150°C to form metal-oleate complexes. A stoichiometric amount of potassium fluoride was then added to a solution of the metal-oleate complexes at room temperature to initiate the crystal growth. Subsequently, the reaction temperature was increased to 290°C to facilitate the growth of the nanocrystals.

Figure 1a shows a typical transmission electron microscopy (TEM) image of the as-synthesized KMnF<sub>3</sub>:Yb/Er (18:2 mol %) nanocrystals with cubic morphology (Figure S1 in the Supporting Information). The high-magnification TEM image of a single KMnF<sub>3</sub>:Yb/Er nanocube shown in Figure 1b reveals lattice fringes of the {110} with a *d* spacing of 0.31 nm, which is typical for cubic KMnF<sub>3</sub> (Figure 1b). Selected-area electron diffraction patterns obtained from the Fourier transform of the high-magnification TEM image confirms single-crystalline cubic phase of the nanocube (Figure 1c). It should be noted that charge balance will be disturbed when the trivalent lanthanide ions are substituted for the Mn<sup>2+</sup> ions in KMnF<sub>3</sub> nanocrystals. To maintain charge balance, either manganese or potassium vacancies are formed (Figure 1d,e). X-ray powder diffraction studies (Figure S2) show peak positions and intensities that can be well indexed in accordance with cubic KMnF<sub>3</sub> crystals (JCPDS file no. 82-1334), which is consistent with TEM analysis of the samples.

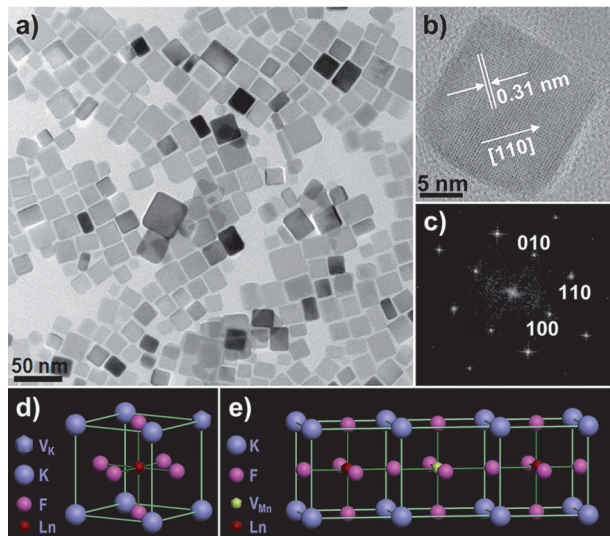


**Figure 1.** a) Low-resolution TEM image of the as-synthesized KMnF<sub>3</sub>:Yb/Er (18:2 mol %) nanocrystals. b) High-magnification TEM image of a single nanocrystal. c) The corresponding Fourier-transform diffraction patterns of the high-magnification TEM image shown in (b). d,e) Schematic representations of lanthanide-doped KMnF<sub>3</sub> cubic structure in form of K<sup>+</sup> and Mn<sup>2+</sup> cation vacancies, respectively.

[\*] J. Wang, Dr. F. Wang, Prof. X. Liu  
Department of Chemistry, National University of Singapore  
3 Science Drive 3, Singapore 117543 (Singapore)

Prof. X. Liu  
Institute of Materials Research and Engineering  
3 Research Link, Singapore 117602 (Singapore)  
E-mail: chmlx@nus.edu.sg

C. Wang, Prof. Z. Liu  
Jiangsu Key Laboratory for Carbon-Based Functional Materials & Devices, Institute of Functional Nano & Soft Materials, Soochow University, Suzhou, Jiangsu, 215123 (P.R. China)

[\*\*] This study was supported in part by the Ministry of Education (MOE2010-T2-083), the Singapore–Peking–Oxford Research Enterprise (SPORE), and the Singapore–MIT alliance. We thank X. Huang and H. Zhu for their help in sample characterization.

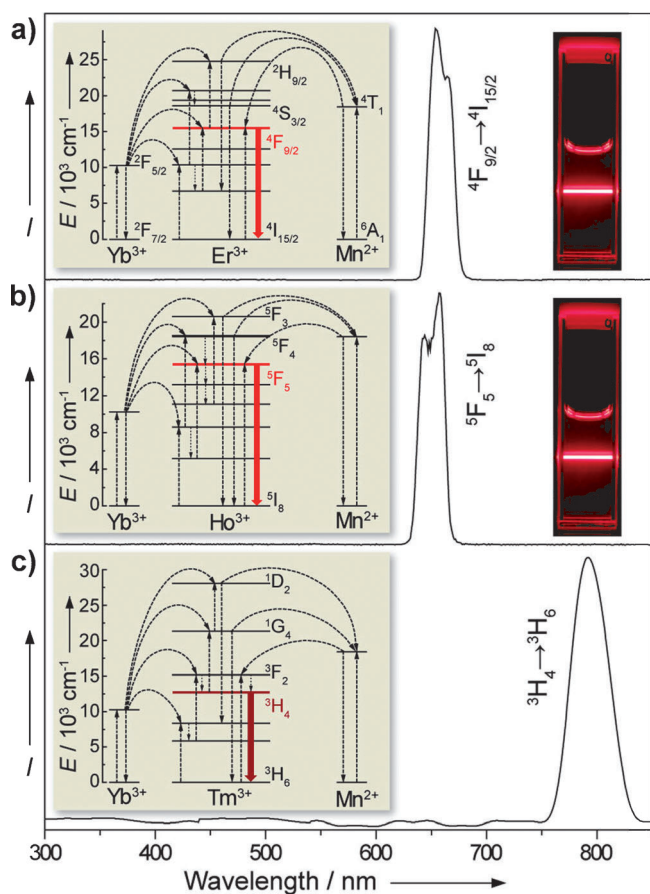
Supporting information for this article is available on the WWW under <http://dx.doi.org/10.1002/anie.201104192>.

Figure 2a displays the room-temperature UC emission spectrum of the irradiated  $\text{KMnF}_3$  nanocrystals. A narrow-band visible emission centered at 660 nm was observed, in stark contrast to  $\text{Yb}^{3+}/\text{Er}^{3+}$  co-doped  $\text{NaYF}_4$  and  $\text{LaF}_3$  nanocrystals, which typically show a set of emission bands in the visible spectral region. The single-band UC emission can be ascribed to nonradiative energy transfer from the  $^2\text{H}_{9/2}$  and  $^4\text{S}_{3/2}$  levels of  $\text{Er}^{3+}$  to the  $^4\text{T}_1$  level of  $\text{Mn}^{2+}$ , followed by back-energy transfer to the  $^4\text{F}_{9/2}$  level of  $\text{Er}^{3+}$  (Figure 2b).<sup>[9c,d]</sup> The complete disappearance of blue and green emissions of  $\text{Er}^{3+}$  suggests an extremely efficient exchange-energy transfer process between the  $\text{Er}^{3+}$  and  $\text{Mn}^{2+}$  ions, which can be largely attributed to the close proximity and effective mixing of wave functions of the  $\text{Er}^{3+}$  and  $\text{Mn}^{2+}$  ions in the crystal host lattices. The low-temperature (10 K) UC emission spectrum of the  $\text{KMnF}_3:\text{Yb}/\text{Er}$  (18:2 mol %) nanocrystals also showed a single-band emission (Figure S3), indicating that the phonon participation in the transfer process has only a marginal effect on the emission. To investigate the compositional effect of the irradiation, we have synthesized  $\text{KMnF}_3$  nanocrystals codoped with  $\text{Yb}^{3+}/\text{Ho}^{3+}$  and  $\text{Yb}^{3+}/\text{Tm}^{3+}$ , respectively. Impor-

tantly, these nanocrystals also displayed single-band emissions involving the  $^5\text{F}_5 \rightarrow ^5\text{I}_8$  transition in  $\text{Ho}^{3+}$  and the  $^3\text{H}_4 \rightarrow ^3\text{H}_6$  transition in  $\text{Tm}^{3+}$  (Figure 2b,c). The full width at half maximum (FWHM) has also been measured to be 20, 23, and 35 nm for  $\text{KMnF}_3:\text{Yb}/\text{Er}$ ,  $\text{KMnF}_3:\text{Yb}/\text{Ho}$ , and  $\text{KMnF}_3:\text{Yb}/\text{Tm}$  nanocrystal systems, respectively.

Significantly, the single-band feature of the  $\text{KMnF}_3:\text{Yb}/\text{Er}$  nanocrystals remained the same on increasing the pump power (Figure 3a). In contrast,  $\text{NaYF}_4:\text{Yb}/\text{Er}$  nanocrystals showed multiplet emissions with relative intensity ratios closely associated with the pump power (Figure 3a). The red emission intensity of the  $\text{KMnF}_3:\text{Yb}/\text{Er}$  nanocrystals was found to be substantially higher than that of the  $\text{NaYF}_4:\text{Yb}/\text{Er}$  nanocrystals of similar particle size irrespective of the pump power (Figure 3b).

In a further set of experiments, we examined the photoluminescence properties of the  $\text{KMnF}_3:\text{Yb}/\text{Er}$  nanocrystals as a function of dopant concentration (Figure S4). As shown in Figure S4a, the  $\text{KMnF}_3$  nanocrystals doped with different amounts of  $\text{Yb}^{3+}/\text{Er}^{3+}$  (0–18:2–5 mol %) all displayed a single-band emission centered at 660 nm, thus confirming the dominant effect of energy transfer process between the  $\text{Er}^{3+}$  and  $\text{Mn}^{2+}$  ions. It is noted that the  $\text{KMnF}_3:\text{Yb}/\text{Er}$  (18:2 mol %) nanocrystals hydrothermally prepared by Li and co-workers show a weak green emission at 540 nm in addition to the dominant 660 nm red emission.<sup>[9b]</sup> We attributed the additional emission band to an insufficient energy transfer process between the  $\text{Er}^{3+}$  and  $\text{Mn}^{2+}$  ions, possibly caused by segregation of dopant ions from the host lattices. The



**Figure 2.** Room-temperature UC emission spectra of solutions containing: a)  $\text{KMnF}_3:\text{Yb}/\text{Er}$  (18:2 mol %), b)  $\text{KMnF}_3:\text{Yb}/\text{Ho}$  (18:2 mol %), and c)  $\text{KMnF}_3:\text{Yb}/\text{Tm}$  (18:2 mol %) nanocrystals in cyclohexane (insets: proposed energy transfer mechanisms and corresponding luminescent photos of the colloidal solutions). All spectra were recorded under excitation of a 980 nm CW diode laser at a power density of  $10 \text{ W cm}^{-2}$ .

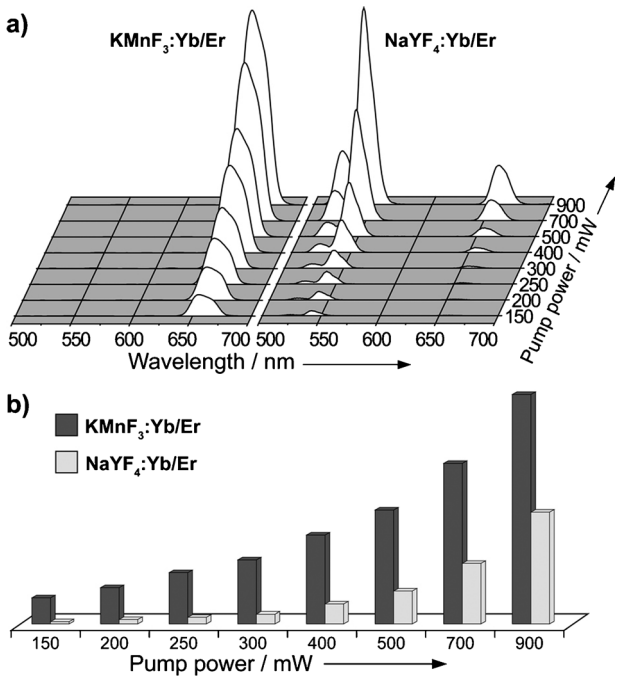


**Figure 3.** a) Pump-power-dependent UC emission spectra of solutions containing  $\text{KMnF}_3:\text{Yb}/\text{Er}$  (18:2 mol %) and  $\text{NaYF}_4:\text{Yb}/\text{Er}$  (18:2 mol %) nanocrystals. All spectra were recorded at room temperature under excitation of a 980 nm CW diode laser at a power density of  $10 \text{ W cm}^{-2}$ . b) Emission intensity comparison of the red emission from the  $\text{KMnF}_3$  and  $\text{NaYF}_4$  nanocrystals as a function of pump power.

segregation of dopant ions is typically observed when divalent host ions are substituted for trivalent lanthanide ions at high concentration.<sup>[11]</sup> To validate this hypothesis, a series of  $\text{KMnF}_3$  samples doped with different concentrations of  $\text{Yb}^{3+}/\text{Er}^{3+}$  were prepared according to the reported hydrothermal method. The nanocrystals with relatively low concentrations of  $\text{Yb}^{3+}/\text{Er}^{3+}$  (9:2 and 0:5 mol %) showed single-band emissions, whereas nanocrystals doped with 18:2 mol %  $\text{Yb}^{3+}/\text{Er}^{3+}$  exhibited similar emission patterns to those previously reported (Figure S4). Taken together, these comparative studies suggest that our oil-based synthetic procedure with controlled stirring enables more homogeneous doping of large lanthanide content into the  $\text{KMnF}_3$  host lattices than the hydrothermal method.

One important application of single-band red-emission  $\text{KMnF}_3:\text{Yb}/\text{Er}$  nanocrystals is the development of suitable luminescent biomarkers for deep tissue labeling and imaging. The emission wavelength of  $\text{KMnF}_3:\text{Yb}/\text{Er}$  nanocrystals falls within the “optical window” in biological tissue, where the emitted light has its maximum depth of penetration.<sup>[12]</sup> As a proof-of-concept experiment, we injected polymer-modified  $\text{KMnF}_3:\text{Yb}/\text{Er}$  nanocrystals into pork muscle tissue at varied depths (0–10 mm) and imaged them by a modified Maestro *in vivo* imaging system. As shown in Figure 4a, the nanocrystals can be visualized even at a depth of 10 mm under an excitation power density of approximately  $0.2 \text{ W cm}^{-2}$ . Under identical experimental settings, however,  $\text{NaYF}_4$  nanocrystals co-doped with  $\text{Yb}^{3+}/\text{Er}^{3+}$  at different ratios can only be detected at about 5 mm beneath the tissue surface (Figure 4b,c). Notably, the emission color of the  $\text{KMnF}_3:\text{Yb}/\text{Er}$  nanocrystals did not change as a function of sample imaging depth, as confirmed by the recorded corresponding emission spectra (Figure 4d). In stark contrast, the  $\text{NaYF}_4$  nanocrystals injected at different depths showed significant changes in emission color, which can be attributed to rapid attenuation of the green emission relative to red emission in tissue (Figure 4e,f).

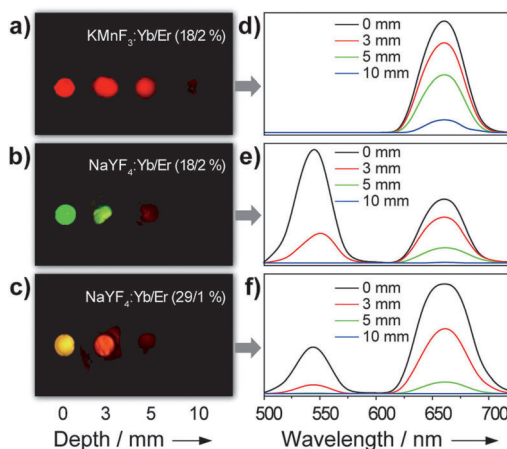


**Figure 4.** Luminescence images of pork muscle tissues injected with different UC nanocrystals. a)  $\text{KMnF}_3:\text{Yb}/\text{Er}$  (18:2 mol %), b)  $\text{NaYF}_4:\text{Yb}/\text{Er}$  (18:2 mol %), c)  $\text{NaYF}_4:\text{Yb}/\text{Er}$  (29:1 mol %). d–f) Corresponding emission luminescence spectra of (a–c). All images and spectra were taken under a 980 nm laser excitation with a power density of approximately  $0.2 \text{ W cm}^{-2}$ . Note that the intensities of the two systems at 0 nm are almost the same.

In conclusion, we have described an oil-based synthetic method for the preparation of  $\text{KMnF}_3$  nanocrystals with lanthanide dopants homogeneously incorporated in the host lattice. As a result of efficient energy transfer between the dopant ion and host  $\text{Mn}^{2+}$  ion, remarkably pure single-band UC emissions were generated in the red and near-infrared spectral regions. The complete lack of short-wavelength emission of these lanthanide-doped nanocrystals in the visible spectral region provides a platform for promising applications in biolabeling studies, for which imaging at different sample depths is required.

## Experimental Section

Reagents:  $\text{MnCl}_2 \cdot 4\text{H}_2\text{O}$  (98 %), potassium oleate,  $\text{YbCl}_3 \cdot 6\text{H}_2\text{O}$  (99.99 %),  $\text{YbCl}_3 \cdot 6\text{H}_2\text{O}$  (99.99 %),  $\text{ErCl}_3 \cdot 6\text{H}_2\text{O}$  (99.9 %),  $\text{TmCl}_3 \cdot 6\text{H}_2\text{O}$  (99.99 %),  $\text{NaOH}$  (98 + %),  $\text{KF}$  (99 + %), 1-octadecene (90 %), oleic acid (90 %), and oleylamine (70 %) were purchased from Sigma–Aldrich. All the chemicals were used as starting materials without further purification.

Synthesis of the lanthanide-doped  $\text{KMnF}_3$  nanocrystals at  $290^\circ\text{C}$ : In a typical procedure to the synthesis of the lanthanide-doped  $\text{KMnF}_3$  nanocrystals, pre-prepared manganese oleate (197.7 mg) precursor<sup>[13]</sup> was added along with  $\text{YbCl}_3$  (0.072 mmol) and  $\text{ErCl}_3$  (0.008 mmol) to a flask containing a mixture of oleylamine (1 mL), oleic acid (1 mL), and 1-octadecene (8 mL) under vigorous stirring at room temperature. The resulting mixture was then heated at  $150^\circ\text{C}$  for 1 h, at which time the solution turned from colorless to yellowish. After the solution was cooled to room temperature, a methanolic solution (2 mL) of  $\text{KF}$  (1.2 mmol) was injected into the flask. The mixture was stirred at  $65^\circ\text{C}$  for 30 min and then purged by nitrogen at  $105^\circ\text{C}$  for 10 min. Subsequently, the temperature was raised to  $290^\circ\text{C}$  and kept for 90 min under nitrogen atmosphere. Finally, the reaction was cooled to room temperature. The as-prepared nanocrystals were collected by centrifugation, washed with ethanol and methanol several times, and finally re-dispersed in cyclohexane.

Imaging of biological samples: Polymer-functionalized<sup>[4m,14]</sup> water-soluble  $\text{KMnF}_3:\text{Yb}/\text{Er}$  ( $10 \text{ mg mL}^{-1}$ ) and  $\text{NaYF}_4:\text{Yb}/\text{Er}$  nanocrystals ( $10 \text{ mg mL}^{-1}$ ) were dissolved in 1 % warm agarose solutions and transferred into a 96-well plate (100  $\mu\text{L}$  for each well). After cooling to the room temperature, the solidified agarose gel plates containing the nanoparticles were taken and placed into pork muscle tissues at different depths (0 mm, 3 mm, 5 mm, and 10 mm). Upconversion luminescence images of pork tissues with nanocrystal gel plates embedded were taken by a modified Maestro *in vivo* imaging system using a 980 nm optical fiber-coupled laser as the excitation source. The laser power density was  $0.2 \text{ W cm}^{-2}$  during imaging. An 850 nm short-pass emission filter was applied to prevent the interference of excitation light to the CCD camera. Spectral imaging from 500 nm to 720 nm (10 nm steps) was carried out with an exposure time of 500 ms for each image frame.

Received: June 17, 2011

Published online: September 14, 2011

**Keywords:** fluorescence · imaging agents · lanthanides · nanostructures

- [1] a) X. Xue, F. Wang, X. Liu, *J. Mater. Chem.* **2011**, *21*, 13107; b) F. Wang, Y. Han, C. S. Lim, Y. H. Lu, J. Wang, J. Xu, H. Y. Chen, C. Zhang, M. Hong, X. Liu, *Nature* **2010**, *463*, 1061; c) Z. Li, L. Li, H. Zhou, Q. Yuan, C. Chen, L. Sun, C. Yan, *Chem. Commun.* **2009**, 6616; d) C. Yan, A. Dadavand, F. Rosei, D. F. Perepichka, *J.*

- Am. Chem. Soc.* **2010**, *132*, 8868; e) N. Liu, W. Qin, G. Qin, T. Jiang, D. Zhao, *Chem. Commun.* **2011**, *47*, 7671; f) H. Zhang, Y. Li, I. A. Ivanov, Y. Qu, Y. Huang, X. Duan, *Angew. Chem.* **2010**, *122*, 2927; *Angew. Chem. Int. Ed.* **2010**, *49*, 2865; g) Z. Li, L. Wang, Z. Wang, X. Liu, Y. Xiong, *J. Phys. Chem. C* **2011**, *115*, 3291; h) F. Zhang, G. B. Braun, Y. Shi, Y. Zhang, X. Sun, N. Reich, D. Zhao, G. Stucky, *J. Am. Chem. Soc.* **2010**, *132*, 2850; i) S. Zhou, N. Jiang, K. Miura, S. Tanabe, M. Shimizu, M. Sakakura, Y. Shimotsuma, M. Nishi, J. Qiu, K. Hirao, *J. Am. Chem. Soc.* **2010**, *132*, 17945; j) C. Jiang, F. Wang, N. Wu, X. Liu, *Adv. Mater.* **2008**, *20*, 4826.
- [2] a) A. Shalav, B. S. Richards, T. Trupke, K. W. Krämer, H. U. Güdel, *Appl. Phys. Lett.* **2005**, *86*, 013505; b) A. Shalav, B. S. Richards, M. A. Green, *Sol. Energy Mater. Sol. Cells* **2007**, *91*, 829; c) S. Ivanova, F. Pellé, *J. Opt. Soc. Am. B* **2009**, *26*, 1930; d) B. M. van der Ende, L. Aarts, A. Meijerink, *Phys. Chem. Chem. Phys.* **2009**, *11*, 11081; e) G. Wang, Q. Peng, Y. Li, *Acc. Chem. Res.* **2011**, *44*, 322.
- [3] a) M. Haase, H. Schäfer, *Angew. Chem.* **2011**, *123*, 5928; *Angew. Chem. Int. Ed.* **2011**, *50*, 5808; b) F. Wang, D. Banerjee, Y. Liu, X. Chen, X. Liu, *Analyst* **2010**, *135*, 1839; c) H. S. Mader, P. Kele, S. M. Saleh, O. S. Wolfbeis, *Curr. Opin. Chem. Biol.* **2010**, *14*, 582; d) J. Shen, L. D. Sun, C. H. Yan, *Dalton Trans.* **2008**, 5687; e) Z. G. Chen, H. L. Chen, H. Hu, M. X. Yu, F. Y. Li, Q. Zhang, Z. G. Zhou, T. Yi, C. H. Huang, *J. Am. Chem. Soc.* **2008**, *130*, 3023; f) M. Nyk, R. Kumar, T. Y. Ohulchanskyy, E. J. Bergey, P. N. Prasad, *Nano Lett.* **2008**, *8*, 3834; g) G. K. Das, T. T. Y. Tan, *J. Phys. Chem. C* **2008**, *112*, 11211; h) G. K. Das, B. C. Heng, S. C. Ng, T. White, J. S. C. Loo, L. D'Silva, P. Padmanabhan, K. K. Bhakoo, S. T. Selvan, T. T. Y. Tan, *Langmuir* **2010**, *26*, 8959; i) G. Jia, H. You, K. Liu, Y. Zheng, N. Guo, H. Zhang, *Langmuir* **2010**, *26*, 5122; j) G. Chen, T. Y. Ohulchanskyy, R. Kumar, H. Agren, P. N. Prasad, *ACS Nano* **2010**, *4*, 3163; k) Z. Wang, J. Hao, H. L. W. Chan, G. L. Law, W. Wong, M. B. Murphy, T. Su, Z. Zhang, S. Zeng, *Nanoscale* **2011**, *3*, 2175; l) P. Ghosh, J. Oliva, E. De La Rosa, K. K. Haldar, D. Solis, A. Patra, *J. Phys. Chem. C* **2008**, *112*, 9650; m) H. Schäfer, P. Ptacek, K. Kömppe, M. Hasse, *Chem. Mater.* **2007**, *19*, 1396; n) Z. Wang, J. Hao, H. L. W. Chan, *J. Mater. Chem.* **2010**, *20*, 3178; o) J. Hao, Y. Zhang, X. Wei, *Angew. Chem.* **2011**, *123*, 7008; *Angew. Chem. Int. Ed.* **2011**, *50*, 6876.
- [4] a) F. Wang, X. G. Liu, *Chem. Soc. Rev.* **2009**, *38*, 976; b) S. Gai, P. Yang, C. Li, W. Wang, Y. Dai, N. Niu, J. Lin, *Adv. Funct. Mater.* **2010**, *20*, 1166; c) Q. Liu, Y. Sun, C. Li, C. Li, J. Zhou, C. Li, T. Yang, X. Zhang, F. Li, *ACS Nano* **2011**, *5*, 3146; d) H. S. Mader, O. S. Wolfbeis, *Anal. Chem.* **2010**, *82*, 5002; e) D. Tu, L. Liu, Q. Ju, Y. Liu, H. Zhu, R. Li, X. Chen, *Angew. Chem.* **2011**, *123*, 6430; *Angew. Chem. Int. Ed.* **2011**, *50*, 6306; f) H. Qian, H. Guo, P. Ho, R. Mahendran, Y. Zhang, *Small* **2009**, *5*, 2285; g) N. M. Idris, Z. Q. Li, L. Ye, E. K. Sim, R. Mahendran, P. C. L. Ho, Y. Zhang, *Biomaterials* **2009**, *30*, 5104; h) C. J. Carling, F. Nourmohammadi, J. C. Boyer, N. R. Branda, *Angew. Chem.* **2010**, *122*, 3870; *Angew. Chem. Int. Ed.* **2010**, *49*, 3782; i) Ref. [3e]; j) T. Cao, Y. Yang, Y. Gao, J. Zhou, Z. Li, F. Li, *Biomaterials* **2011**, *32*, 2959; k) J. Zhou, M. Yu, Y. Sun, X. Zhang, X. Zhu, Z. Wu, D. Wu, F. Li, *Biomaterials* **2011**, *32*, 1148; l) X. Yu, L. Chen, M. Li, M. Xie, L. Zhou, Y. Li, Q. Wang, *Adv. Mater.* **2008**, *20*, 4118; m) C. Wang, L. Cheng, Z. Liu, *Biomaterials* **2011**, *32*, 1110; n) C. Wang, H. Tao, L. Cheng, Z. Liu, *Biomaterials* **2011**, *32*, 6245; o) L. H. Fischer, G. S. Harms, O. S. Wolfbeis, *Angew. Chem.* **2011**, *123*, 4640; *Angew. Chem. Int. Ed.* **2011**, *50*, 4546.
- [5] a) J. Wang, F. Wang, J. Xu, Y. Wang, Y. Liu, X. Chen, H. Chen, X. Liu, *C. R. Chim.* **2010**, *13*, 731; b) F. Wang, J. Wang, X. Liu, *Angew. Chem.* **2010**, *122*, 7618; *Angew. Chem. Int. Ed.* **2010**, *49*, 7456; c) F. Wang, J. Wang, J. Xu, X. Xue, H. Chen, X. Liu, *Spectrosc. Lett.* **2010**, *43*, 400; d) F. Heine, E. Heumann, T. Danger, T. Schweizer, G. Hüber, *Appl. Phys. Lett.* **1994**, *65*, 383; e) T. Sandrock, H. Scheife, E. Heumann, G. Huber, *Opt. Lett.* **1997**, *22*, 808; f) C. Chen, L. D. Sun, Z. X. Li, L. L. Li, J. Zhang, Y. W. Zhang, C. H. Yan, *Langmuir* **2010**, *26*, 8797; g) F. Zhang, Y. Wan, T. Yu, F. Zhang, Y. Shi, S. Xie, Y. Li, L. Xu, B. Tu, D. Zhao, *Angew. Chem.* **2007**, *119*, 8122; *Angew. Chem. Int. Ed.* **2007**, *46*, 7976; h) W. Niu, S. Wu, S. Zhang, *J. Mater. Chem.* **2010**, *20*, 9113; i) G. Wang, Q. Peng, Y. Li, *Chem. Eur. J.* **2010**, *16*, 4923; j) K. A. Abel, J. C. Boyer, F. C. J. M. van Veggel, *J. Am. Chem. Soc.* **2009**, *131*, 14644; k) N. M. Sangeetha, F. C. J. M. van Veggel, *J. Phys. Chem. C* **2009**, *113*, 14702; l) D. Q. Chen, Y. L. Yu, F. Huang, P. Huang, A. P. Yang, Y. S. Wang, *J. Am. Chem. Soc.* **2010**, *132*, 9976; m) D. Q. Chen, Y. L. Yu, F. Huang, Y. S. Wang, *Chem. Commun.* **2011**, *47*, 2601; n) J. C. Boyer, L. A. Cuccia, J. A. Capobianco, *Nano Lett.* **2007**, *7*, 847; o) J. C. Boyer, J. Gagnon, L. A. Cuccia, J. A. Capobianco, *Chem. Mater.* **2007**, *19*, 3358; p) V. Mahalingam, R. Naccache, F. Vetrone, J. A. Capobianco, *Chem. Eur. J.* **2009**, *15*, 9660; q) G. S. Yi, G. M. Chow, *Chem. Mater.* **2007**, *19*, 341; r) G. S. Yi, G. M. Chow, *Adv. Funct. Mater.* **2006**, *16*, 2324; s) G. Yi, Y. Peng, Z. Gao, *Chem. Mater.* **2011**, *23*, 2729; t) C. H. Liu, D. P. Chen, *J. Mater. Chem.* **2007**, *17*, 3875; u) W. Niu, S. Wu, S. Zhang, L. Li, *Chem. Commun.* **2010**, *46*, 3908; v) X. Ye, J. Collins, Y. Kang, J. Chen, D. T. N. Chen, A. G. Yodh, C. B. Murray, *Proc. Natl. Acad. Sci. USA* **2010**, *107*, 22430; w) H. Q. Wang, T. Nann, *ACS Nano* **2010**, *3*, 3804.
- [6] a) G. Blasse, B. C. Grabmaier, *Luminescent materials*, Springer, Berlin, **1994**; b) J. F. Suyver, J. Grimm, K. W. Krämer, H. U. Güdel, *J. Lumin.* **2005**, *114*, 53; c) G. He, P. P. Markowicz, T. Lin, P. N. Prasad, *Nature* **2002**, *415*, 767; d) F. Auzel, *Chem. Rev.* **2004**, *104*, 139; e) Ref. [5t].
- [7] W. Song, A. E. Vasdekis, Z. Li, D. Psaltis, *Appl. Phys. Lett.* **2009**, *94*, 051117.
- [8] a) F. Wang, X. Liu, *J. Am. Chem. Soc.* **2008**, *130*, 5642; b) J. Zhao, Y. Sun, X. Kong, L. Tian, Y. Wang, L. Tu, J. Zhao, H. Zhang, *J. Phys. Chem. B* **2008**, *112*, 15666.
- [9] a) M. Xie, X. Peng, X. Fu, J. Zhang, G. Li, X. Yu, *Scr. Mater.* **2009**, *60*, 190; b) J. Zeng, T. Xie, Z. Li, Y. Li, *Cryst. Growth Des.* **2007**, *7*, 2774; c) D. D. Sell, R. L. Greene, R. M. White, *Phys. Rev.* **1967**, *158*, 489; d) J. M. Flaherty, B. D. Bartolo, *J. Lumin.* **1973**, *8*, 51.
- [10] H. X. Mai, Y. W. Zhang, L. D. Sun, C. H. Yan, *Chem. Mater.* **2007**, *19*, 4514.
- [11] a) Y. Vaills, J. Y. Buzare, M. Rousseau, *J. Phys. Condens. Matter* **1990**, *2*, 3997; b) J. L. Patel, J. J. Davies, B. C. Cavenett, *J. Phys. C* **1976**, *9*, 129.
- [12] a) K. König, *J. Microsc.* **2000**, *200*, 83; b) R. G. Aswathy, Y. Yoshida, T. Maekawa, D. S. Kumar, *Anal. Bioanal. Chem.* **2010**, *397*, 1417.
- [13] J. Park, K. An, Y. H. J. G. Park, H. J. Noh, J. Y. Kim, J. H. Park, N. M. Hwang, T. Hyeon, *Nat. Mater.* **2004**, *3*, 891.
- [14] L. Cheng, K. Yang, S. Zhuang, M. W. Shao, S. T. Lee, Z. Liu, *Nano Res.* **2010**, *3*, 676.